*Article*

# Quadruple-U Auxiliary Structure-Based Receiving Coil Positioning System for Electric Vehicle Wireless Charger

**Chuan Li, Yi Yang and Guimei Cao ***

School of Electrical and Electronic Engineering, Chongqing University of Technology, Chongqing 400054, China; lichuan@cqut.edu.cn (C.L.); yangyi@cqut.edu.cn (Y.Y.)
**\*** Correspondence: cgm0121@163.com; Tel.: +86-17774983076

**Abstract:** In order to strike a balance between economic development and green travel, electric vehicles with wireless charging have become one of the first choices for future transportation. Misalignment between the transmitting coil and receiving coil in wireless charging systems decreases power capacity and efficiency to a great extent. Hence, the detection of whether the electric vehicle enters the effective charging area is a hot issue in the current research. In this paper, a receiving coil positioning approach integrated with a quadruple-U auxiliary structure is proposed. The designed quadruple-U auxiliary structure with cruciform distribution consists of four U-shaped coils, which are inspired by the solenoid coil. Based on the symmetry of the auxiliary structure, a receiving coil positioning method is proposed by measuring the load voltages of each U-shaped coil working independently. Coordinates can be obtained by retrieving the measured results with the database established in advance. The positioning method has the advantages of wider positioning ranges, higher positioning accuracy, and not changing the structure of the receiving coil. Furthermore, the specific magnetic coupler is simulated by a three-dimensional finite element modeling tool and was verified by an experiment on a prototype. During the positioning process, the positions distributed throughout the $\Delta X \in [-300 \text{ mm}, 0 \text{ mm}] \cap \Delta Y \in [-300 \text{ mm}, 300 \text{ mm}]$ positioning range were tested. The experimental results indicate that all of the tested positions are accurate to within 10 mm, with a 160 mm transfer distance. Meanwhile, combined with the symmetry of the auxiliary structure and the test results, it can be indicated that the positioning range can reach $\Delta X \in [-300 \text{ mm}, 300 \text{ mm}] \cap \Delta Y \in [-300 \text{ mm}, 300 \text{ mm}]$.

**Keywords:** wireless charging; quadruple-U auxiliary structure; receiving coil positioning

## 1. Introduction

With the proposal of carbon peaking and carbon neutrality goals [1], wireless power transfer technology (WPT) has received extensive attention from more and more experts and scholars for its unique energy transmission form, green and environmental protection [2], safety, and adaptability [3]. Compared with the rapid rise of WPT in consumer electronics, medical products, smart kitchens, and other low-power applications [4], its research and application in the field of transportation are still in the development stage. Hence, to strike a balance between economic development and green travel, electric vehicles with wireless charging have become one of the first choices for future transportation [5]. In the electric vehicle WPT system, the detection of whether it is in the effective charging area is the current critical issue to be addressed.

Early detection approaches are mainly realized by utilizing commonly used sensors, such as RFID [6], GPS [7], UWB [8], and so on. However, these approaches either require installing the electronic tags in advance, which increases the system's maintenance cost, or just roughly navigating the vehicle. In order to address these limitations, the existing research is prone to positioning the vehicle through three novel methods, which are utilizing the characteristic of the magnetic coupler, changing the structure of the coils, and adding the auxiliary coil.

Aiming at avoiding the complexity of the WPT system caused by additional sensors, Southeast University proposed a receiving coil positioning approach by combining the nonlinear relation with the backpropagation (BP) neural network [9]. The former is the relationship that the induced voltage varies with the relative position between the two power transfer coils, and the latter can be used to effectively fit the nonlinear equation. It is proved that this approach can be used to achieve positioning within the centimeter range. In addition, considering the uncertainty of the data fitting method adopted to position the receiving coil, Southwest Jiaotong University obtained the coil self-positioning approach by deducing the mathematical relationship between mutual inductance and the coils' position [10]. This approach is used for deciding the spatial coordinate of the transmitting coil, and it is worth mentioning that the positioning accuracy of it can reach 1 mm. Although these positioning methods based on the characteristic of the magnetic coupler can effectively eliminate the complexity of the system, it has limitations for just applicable to the specific magnetic coupler, such as circular or rectangular.

It is generally known that shortening the transmission distance can enhance the transmission efficiency and power of the system substantially [11]. Hence, the University of Toronto proposed a compact WPT charging system located at the rear of a vehicle and designed a closed-loop control algorithm for vehicle positioning based on the impedance and resonant frequency of the system [12]. However, this approach not only radically changes the magnetic coupler but also needs to install additional rails to accommodate the movement of the transmitting coil. Meanwhile, approaches through changing the magnetic coupler's structure to positioning the receiving coil are commonly used, such as the orthogonal decoupled magnetic coupler consisting of a double-D (DD) coil and flat solenoid coil [13], the octagon coil derived from the square coil [14], and the reticulated transmitting coil configured by four staggered overlapping curved coils [15], etc. It is obvious that even though the above research has certain innovations, it is hard to replace the magnetic coupler commonly used in the market with these special structures.

Hence, more and more researchers pay attention to the receiving coil positioning approach by adding the auxiliary coil. In order to realize both metal detection and position identification of the WPT system, the Korea Advanced Institute of Science and Technology (KAIST) designed a group of non-overlapping coils placed on the transmitting side [16]. In this system, the position of the vehicle is determined by the induced voltages of the non-overlapping coil group. In addition, the advantage of this approach is that the auxiliary structure has little influence on the transmission efficiency and power of the WPT system. For the issue of the complicated volume caused by the installation of an auxiliary coil in the WPT system, a specific auxiliary structure has been proposed by Gao, which is four circular coils with tiny radiuses that are symmetrically embedded in a circular receiving coil [17]. Similarly, the achievement of receiving coil positioning also relies on the relationship between the accurate position of the vehicle and the induced voltages of the auxiliary coils. However, the auxiliary coils are too small to position the vehicle with a large transmission distance. In addition, the detection approaches of placing four induced coils at the periphery of the receiving coil are extensively adopted by researchers, as well [18], and the principle of it is to obtain the space coordinates of the vehicle by combining the induced voltage and the fitting curve [19]. It can be indicated that these approaches involve changing the structure of the receiving coils, which prompts it difficult to be applied to the industrialization of electric vehicle WPT systems.

In conclusion, even if plenty of vehicle positioning approaches have been introduced, there still exist quite a few crucial issues that need to be further studied. The characteristics of existing positioning methods are listed in Table 1. It follows that how fulfilling the vehicle positioning relies on maintaining the magnetic coupler's structure as far as possible is a vital problem in the development of the electric vehicle WPT system. At present, placing the auxiliary coil on the primary side can tackle this issue effectively. Considering the realistic requirements for vehicle positioning, including high precision, a wide identification range, maintaining the original structure, and no influence on the transmission efficiency, we

designed a novel auxiliary structure consisting of four U-shaped coils, which are inspired by the solenoid coil.

**Table 1.** Characteristics of existing positioning methods.

| Method | Advantage | Disadvantage |
| :---: | :---: | :---: |
| Use sensor | Simplify the positioning process | Increase the cost |
| Use the coil's parameters | High positioning accuracy | Lack of applicability |
| Use new magnetic coupler | Satisfactory accuracy | Lack of practicality |
| Place the auxiliary coil on the secondary side | Satisfactory accuracy | Change the receiving coil |
| Place the auxiliary coil on the primary side | Satisfactory accuracy | Change the primary-side |

Compared to the existing methods, the main contributions of this paper are summarized as follows.

(1) A quadruple-U auxiliary structure with cruciform distribution was designed without changing the magnetic coupler;
(2) The magnetic field variation was studied when the proposed quadruple-U auxiliary structure was introduced into the typical magnetic coupler, of which the transmitting coil and the receiving coil are rectangular;
(3) A corresponding positioning approach based on the quadruple-U auxiliary structure was proposed to assist in the vehicle entering the effective charging area.

The rest of this article is organized as follows. The quadruple-U auxiliary structure is presented in Section 2. Circuit modeling and analysis are given in Section 3. The magnetic field variation and the specific positioning approach are described in Section 4. In Section 5, the experimental results for vehicle positioning are obtained from a prototype. Finally, Section 6 concludes this article.

## 2. Auxiliary Structure and Performance

### 2.1. Quadruple-U Auxiliary Structure

The proposed quadruple-U auxiliary structure is located on the primary side, as shown in Figure 1. In Figure 1a, the four identical U-shaped coils marked in red are the main components of this structure, and the transmitting coil is located directly above the quadruple-U auxiliary structure, which is not shown for the positioning process, as it does not involve it. In Figure 1b, the U-shaped coil was inspired by the solenoid coil, and the purpose of modification was to enhance the height of its vertical magnetic field while maintaining its wide horizontal magnetic field range [20].



(a)                                                    (b)
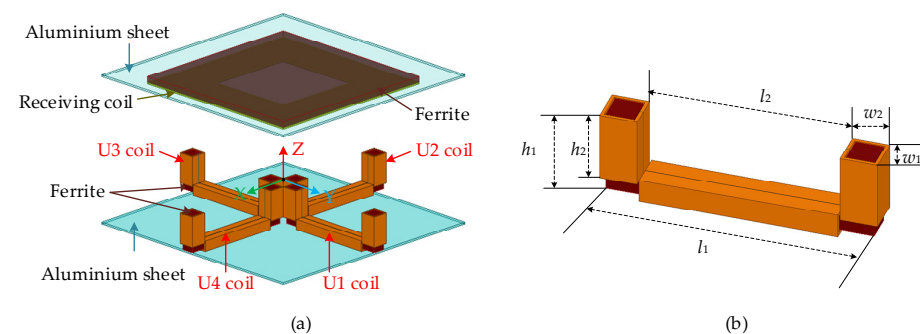
**Figure 1.** Structure of the quadruple-U auxiliary device. (**a**) The overall view. (**b**) The structure of the U-shaped coil.

The magnetic field of the positioning auxiliary structure located on the ground transmitting side should have the characteristics of good height, wide range, and obvious misalignment sensitivity. As is known to all, the magnetic field height of the DD coil is twice that of the circular coil, which is more suitable for the occasion of large transmission distances. Hence, the magnetic field variations of the DD coil and the U-shaped coil under the condition that the overall length of the coil is the same were analyzed, respectively, and the corresponding magnetic field variations are shown in Figure 2.



(a) DD coil             (b) U-shaped coil
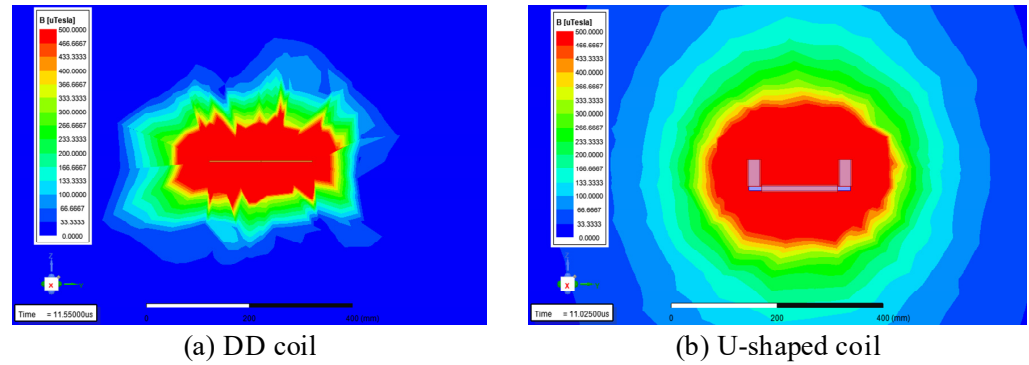
**Figure 2.** Magnetic field variations of the DD coil and the U-shaped coil. (**a**) DD coil. (**b**) U-shaped coil.

It can be seen that the magnetic field height of the DD coil is about half of the length of the coil, while that of the U-shaped coil is about three-fifths of the length of the coil. Meanwhile, the magnetic field variation range of the two coils is almost the same. Moreover, it is worth noting that the magnetic field of the U-shaped coil varies more regularly, which indicates that its misalignment sensitivity can fulfill the actual positioning acquirements perfectly. In addition, combined with the specific structures of each coil, we can find that the structure of the DD coil is too large to be used as an auxiliary coil. Thus, the designed U-shaped coil can meet the practical requirements of positioning the receiving coil both in terms of magnetic field characteristics and structural characteristics. Furthermore, according to the magnetic field characteristics of the U-shaped coil and the actual parking process of the electric vehicle, a quadruple-U auxiliary structure with cruciform distribution was designed.

The auxiliary structure designed in this paper is used to assist the vehicle in entering the effective charging area. Hence, it works in the stage of vehicle positioning, that is, before the system carries out the process of energy transmission. When the system is under the stage of positioning, the four U-shaped coils compose corresponding energy transmission paths with the receiving coil, respectively, which is thanks to the four U-shaped coils working independently. Although the power transfer on each path is much smaller than that in the energy transmission state, it is perfectly adequate for vehicle positioning and guidance. In addition, parameter $M_{R1}$ is defined as the mutual inductance between the U1 coil and the receiving coil. A similar notation applies to the mutual inductances $M_{R2}$, $M_{R3}$, and $M_{R4}$.

Figure 3 presents the simulation results that the mutual inductance between the U-shaped coil and the rectangular receiving coil ($M_{R-U}$) varies with the misalignment position of the receiving coil under the condition that the system is in the positioning and guidance process. It can be seen that the numerical values of $M_{R-U}$ appear the trend as a wavy pattern; that is, $M_{R-U}$ reaches a maximum at $\Delta Y = \pm 100$ mm and approximately zero at $\Delta Y = 0$ mm. Meanwhile, its misalignment sensitivity is satisfactory. The reason is that the U-shaped coil can be regarded as a bipolar coil, while the receiver coil is a unipolar coil. Hence, the mutual inductance between them will present the maximum when the receiver coil is located directly above the two structural endpoints of the U-shaped coil and present approximate zero when it is located directly above the structure center of the U-shaped coil, for they are decoupled from each other.
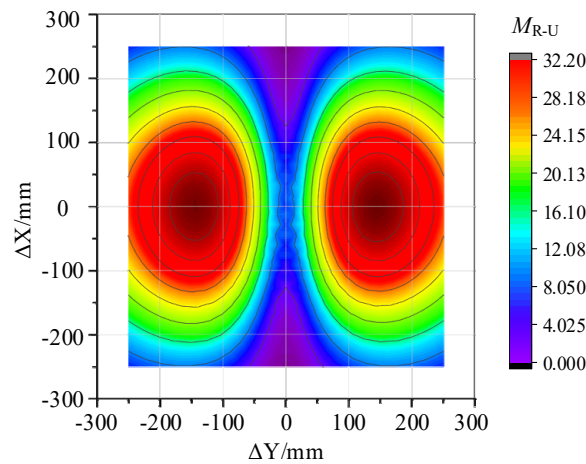
**Figure 3.** $M_{R\text{-}U}$ varies with ΔX and ΔY.

## 2.2. Optimization of the Structural Parameters

Unlike the magnetic coupler used for energy transmission seeking to maximize the quality factor and coupling coefficient, the auxiliary structure strives for significant misalignment sensitivity. Meanwhile, its structural parameters should be optimized under the limitation of available space. Hence, we determined the optimal auxiliary structure by analyzing and comparing the variation of the mutual inductance varying with the dimensional parameters marked in Figure 1b, such as the outer, $l_1$, outer height, $h_1$, outer width, $w_1$, endpoint length, $w_2$, inner height, $h_2$, and inner length, $l_2$. Moreover, we achieved parameter optimization by relying on the following set conditions: the overall dimensions of the primary and the secondary coils and corresponding ferrite are 300 mm × 300 mm, and the transfer distance is 160 mm.

Figure 4 illustrates that the mutual inductance, $M_{R1}$, varies with each crucial parameter when the receiving coil is only misaligned in the *Y*-axis, with the step being 50 mm. As a whole, $M_{R1}$ changes under the influence of any parameter, which is consistent with the trend shown in Figure 2.
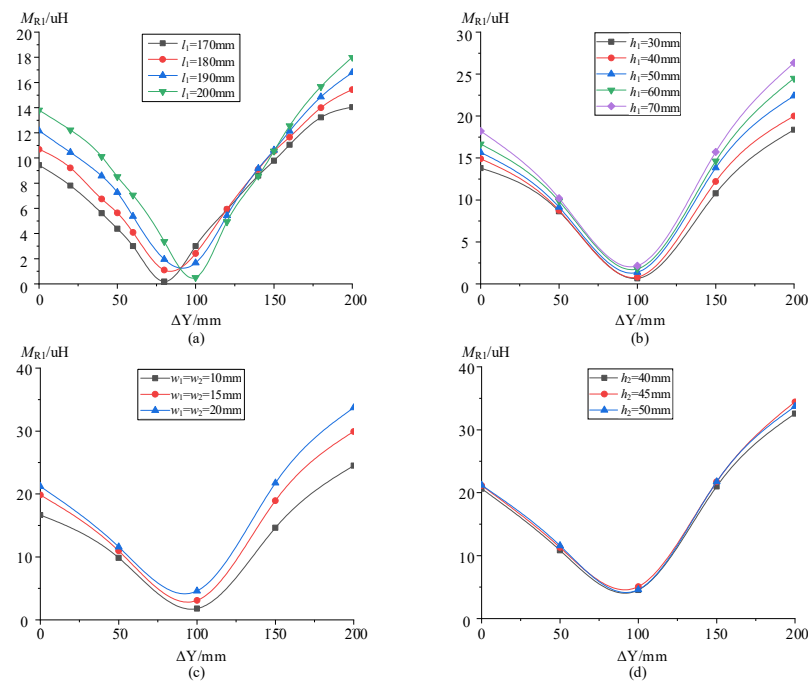


**Figure 4.** Optimization of the structural parameters. (**a**) is the optimization of $l_1$. (**b**) is the optimization of $h_1$. (**c**) is the optimization of $w_1$ and $w_2$. (**d**) is the optimization of $h_2$.

As shown in Figure 4a, we can illustrate that when $\Delta Y < 0.5l_1$, $M_{R1}$ is proportional to $l_1$, and $M_{R1}$ reaches a minimum at $\Delta Y = 0.5l_1$. While the variation of $M_{R1}$, with the change of $l_1$ when $\Delta Y > 0.5l_1$, is not obvious enough. Meanwhile, considering the identifiable range of the U-shaped coil should be enhanced as far as possible under the limitation of the available space, we selected $l_1 = 200$ mm, eventually. In addition, due to the cruciform distribution of the quadruple-U auxiliary structure, one endpoint of each U-shaped coil near the center of the quadruple-U structure will be coupled with the other U-shaped coils, resulting in the variation not being completely symmetric. In order to analyze the influence of $h_1$ on $M_{R1}$, $h_1 - h_2 = 10$ mm was set in this simulation process. As shown in Figure 4b, $M_{R1}$ is proportional to $h_1$, and the numerical value of $M_{R1}$ under the two conditions of $h_1 = 60$ mm and $h_1 = 70$ mm changes little when $\Delta Y$ is within 50 mm~100 mm. Therefore, we picked $h_1$ as equal to 60 mm. Furthermore, in order to simplify the production of the U-shaped coils, we set the parameters $w_1 = w_2$ and optimized them synchronously; the simulation results are shown in Figure 4c. It can be indicated that $M_{R1}$ is also proportional to $w_1$ and $w_2$, while $w_1 = w_2 = 15$ mm and $w_1 = w_2 = 20$ mm have little influence on the variation of $M_{R1}$ when $\Delta Y = 0 \sim 100$ mm. Thus, $w_1 = w_2 = 15$ mm was determined. At last, the variation between $M_{R1}$ and $h_2$ is exhibited in Figure 4d, and it can be seen that even if $h_2$ changes, it has little effect on $M_{R1}$. Therefore, $h_2 = 50$ mm was selected to reduce the volume of the ferrite.

By introducing the proposed auxiliary structure into the original magnetic coupler to optimize the U-coil, the satisfactory misalignment sensitivity of the structure can be achieved on the basis of maximizing the utilization of available space, which provides feasibility for the subsequent receiving coil positioning and guiding of the structure.

## 3. WPT System Based on the Quadruple-U Auxiliary Structure

### 3.1. Positioning System Model

The wireless charging positioning system with the symmetrical auxiliary structure is mainly composed of the ground auxiliary side and the vehicle receiving side. For the specific structure, there exists a certain coupling relationship between each U-shaped auxiliary coil and the receiving coil when the receiving coil is misaligned. Combined with the coupling between the coils, the circuit topology of the positioning system can be obtained, as shown in Figure 5.
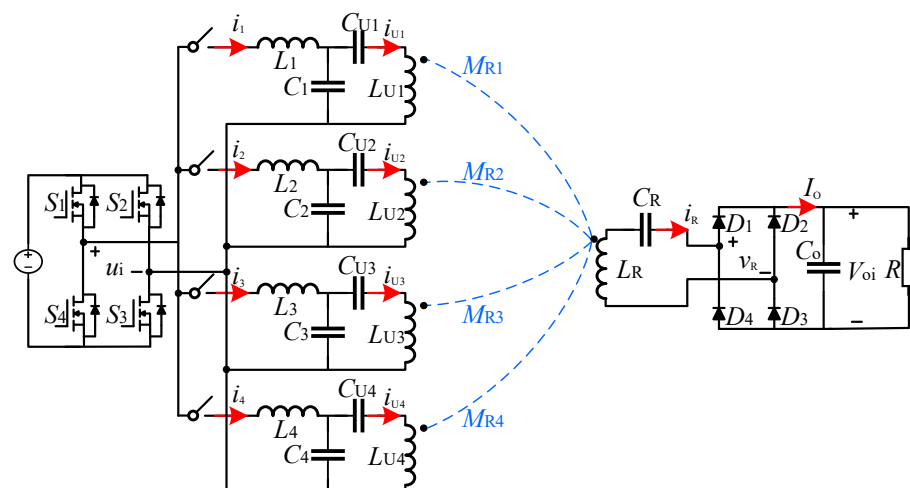


**Figure 5.** Circuit topology of the positioning system with the auxiliary structure.

In Figure 5, $S_1-S_4$ is the switch of the full-bridge inverter circuit, and $D_1-D_4$ is the diode of the rectifier circuit. $L_R$, $L_{U1}$, $L_{U2}$, $L_{U3}$, and $L_{U4}$ represent the inductance of the receiving coil and the four auxiliary coils. $C_R$, $C_{U1}$, $C_{U2}$, $C_{U3}$, and $C_{U4}$ represent the resonant capacitor in the series of the corresponding inductance. $L_1$, $L_2$, $L_3$, $L_4$, and $C_1$, $C_2$, $C_3$, and $C_{U4}$ are the other compensating inductances and compensating capacitances, respectively,

in the LCC resonant circuit at the transmitting side. $M_{R1}$, $M_{R2}$, $M_{R3}$, and $M_{R4}$ are the mutual inductances between each U-shaped coil and the reserving coil. Moreover, due to the method that four U-shaped coils worked independently was adopted to avoid the influence of the complex cross-coupling situation on the system, the other mutual inductances, such as between one U-shaped coil and another, $M_{12}$, $M_{13}$, $M_{14}$, $M_{23}$, $M_{24}$, and $M_{34}$ are not shown.

When the system is in the positioning stage, the frequency control method is used to make each U-coil work independently and turn off the switch connecting the inverter and the transmitting coil. Meanwhile, considering that the transmission efficiency of the magnetic coupler would be affected when the system deviated from the resonant frequency, the switching frequency of the four U-shaped coils was set as 94 kHz, 94.5 kHz, 95.5 kHz, and 96 kHz, and the coupling frequency of the system was 95 kHz. Take one of the U-shaped coil operations as an example. The corresponding equivalent circuit is shown in Figure 6.
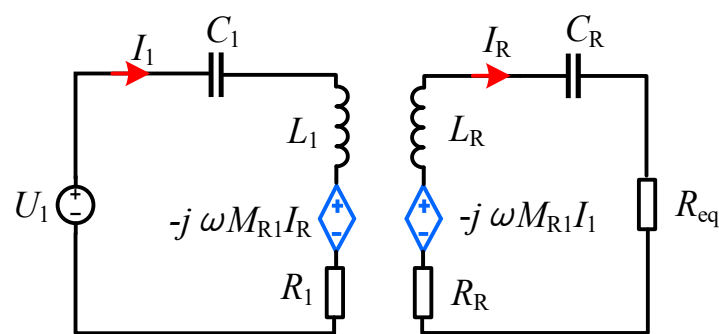


**Figure 6.** Equivalent circuit.

Based on Kirchhoff's law and circuit resonance conditions, the loop currents are:

$$\begin{cases} I_1 = \frac{(R_{eq}+R_R)U_1}{M^2\omega^2+R_1(R_{eq}+R_R)} \\ I_R = \frac{jM\omega U_1}{M^2\omega^2+R_1(R_{eq}+R_R)} \end{cases} \tag{1}$$

It can be seen that the output current and voltage just depend on the mutual inductance between the U-shaped coil and the receiving coil when the inherent parameters of the system are known. Therefore, the analytical relationship between the mutual inductance and the misaligned extent of the receiving coil is crucial to realize the receiving coil's positioning.

### 3.2. Calculation of Mutual Inductance

The mutual inductance between two coils is calculated according to the Neumann formula [21]:

$$M_{R-U} = \frac{\mu_0}{4\pi} \oint_{l1} \oint_{l2} \frac{dl_1 \bullet dl_2}{r} \tag{2}$$

where the $M_{R\text{-}U}$ represents the mutual inductance between the receiving coil and U-shaped coil, $\mu_0$ is the vacuum permeability, and $dl_1$ and $dl_2$ indicate the line elements of the corresponding loop [22].

The relative position of the U-shaped coil and rectangular receiving coil in a three-dimensional space are shown in Figure 7. In addition, the U-shaped coil belongs to a tightly wound solenoid coil [23], and its magnetic core section is rectangular, so each turn can be an approximately closed rectangular current [24].
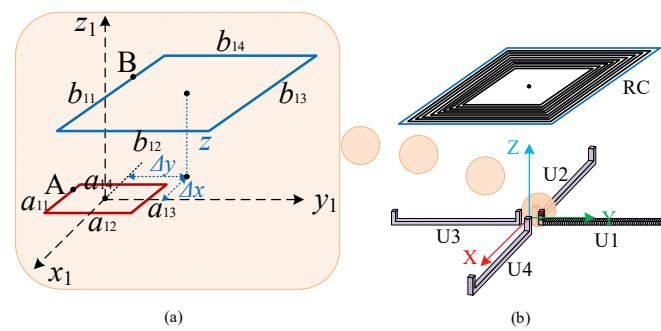
**Figure 7.** Relative position of U-shaped coil and rectangular receiving coil. (**a**) Relative position between two single-turn coils. (**b**) Relative position between U-shaped coil and rectangular coil.

The mutual inductance between two single-turn square coils can be equivalent to the superposition of the mutual inductance between each wire segment of them [25], so the mutual inductance calculation method can be expressed as [26]:

$$M_{R-R} = M_{a11-b11} + M_{a11-b13} + M_{a12-b12} + M_{a12-b14} + M_{a13-b11} + M_{a13-b13} + M_{a14-b12} + M_{a14-b14} \tag{3}$$

Taking the calculation of $M_{a11\text{-}b11}$ as an example, the coordinates of any point on the side of $a_{11}$ can be expressed as A($x_1$, $y_1$, 0), and any point on $b_{11}$ is described as B($x_2 + \Delta x$, $y_2 + \Delta y$, $z_1$). Thus, the relative position of the two points can be obtained:

$$\left| \vec{r_1} - \vec{r_2} \right| = \sqrt{[x_1 - (x_2 + \Delta x)]^2 + [y_1 - (y_2 + \Delta y)]^2 + z_1^2} \tag{4}$$

Therefore, the mutual inductance $M_{a11\text{-}b11}$ between $a_{11}$ and $b_{11}$ is:

$$M_{a11-b11} = \frac{\mu_0}{4\pi} \int_{a_{11}} \int_{b_{11}} \frac{dl_1 \bullet dl_2}{\left| \vec{r_1} - \vec{r_2} \right|}$$

$$= \frac{\mu_0}{4\pi} \int_{-\frac{a_{11}}{2}}^{\frac{a_{11}}{2}} \int_{-\frac{b_{11}}{2}}^{\frac{b_{11}}{2}} \frac{dl_1 \bullet dl_2}{\sqrt{[x_1 - (x_2 + \Delta x)]^2 + [y_1 - (y_2 + \Delta y)]^2 + z_1^2}} \tag{5}$$

Furthermore, combined with the specific structural parameters of the two coils shown in Figure 8, where the wire diameter is $r$, the turn spacing of the U-shaped coil is $d_U$, and that in the rectangular coil is $d_R$. The U-shaped coil can be divided into three parts, that is the left vertical sub-coil (20 turns), the lower horizontal sub-coil (60 turns), the right vertical sub-coil (20 turns), and the mutual inductance between the three parts of the U-shaped coil, and the receiving coil is, respectively, expressed as $M_{1(R\text{-}U)}$, $M_{2(R\text{-}U)}$, and $M_{3(R\text{-}U)}$. On the basis of it, the overall mutual inductance can be subdivided into the sum of the mutual inductance between each sub-coil and the receiving coil.
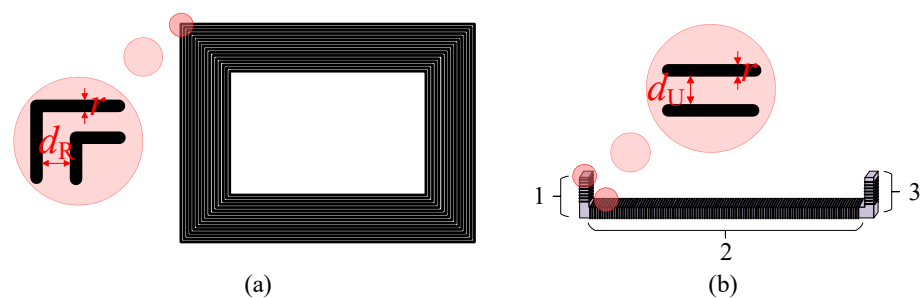


**Figure 8.** Structural parameters of the receiving coil and the U-shaped coil. (**a**) Parameters of the receiving coil. (**b**) Parameters of the U-shaped coil.

In order to simplify the calculation, the sub-coordinate $x_1y_1z_1$ is established at the vertex center of the vertical sub-coil on the left of the U-shaped coil. Any point on the side of $a_{n1}$ can be expressed as A$(x_1, y_1, n \cdot d_U + n \cdot r - d_U - r)$, where $n \in [1,20]$, and any point on the side of $b_{k1}$ is B$(x'_1, y'_1 + k \cdot d_R + k \cdot r - d_R - r, z_1)$, where $k \in [1,20]$. Thus, the mutual inductance between $a_{n1}$ and $b_{n1}$ $M_{1(an1\text{-}bk1)}$ can be obtained.

$$
\begin{cases}
M_{1(a_{n1}-b_{k1})} = \sum_{n=1}^{20}\sum_{k=1}^{20}\frac{\mu_0}{4\pi}\int_{-\frac{a_{n1}}{2}}^{\frac{a_{n1}}{2}}\int_{-\frac{b_{k1}}{2}}^{\frac{b_{k1}}{2}}\frac{dl_1\bullet dl_2}{\sqrt{\left[x_1-(x'_1+\Delta x)\right]^2+\Delta_1^2+[z_1+(n-1)(d_U+r)]^2}} \\
\Delta_1 = y_1 - \left[y'_1 + (k-1)(d_R+r)\right]
\end{cases}
\tag{6}
$$

Similarly, the $M_{2(a_{n1}-b_{k1})}$ and $M_{3(a_{n1}-b_{k1})}$, which are the mutual inductances between the horizontal sub-coil below the U-shaped coil and the vertical sub-coil on the right side, and the $b_{k1}$, respectively [27], can be written as:

$$
\begin{cases}
M_{2(a_{m1}-b_{k1})} = \sum_{m=1}^{60}\sum_{k=1}^{20}\frac{\mu_0}{4\pi}\int_{-\frac{a_{n1}}{2}}^{\frac{a_{n1}}{2}}\int_{-\frac{b_{k1}}{2}}^{\frac{b_{k1}}{2}}\frac{dl_1\bullet dl_2}{\sqrt{\left[x_2-(x'_2+\Delta x)\right]^2+(y_2-y'_2)^2+\Delta_2^2}} \\
\Delta_2 = (m-1)(d_U+r) - \left[(z'_2+\Delta z) - (k-1)(d_R+r)\right]
\end{cases}
\tag{7}
$$

$$
\begin{cases}
M_{3(a_{j1}-b_{k1})} = \sum_{j=1}^{20}\sum_{k=1}^{20}\frac{\mu_0}{4\pi}\int_{-\frac{a_{n1}}{2}}^{\frac{a_{n1}}{2}}\int_{-\frac{b_{k1}}{2}}^{\frac{b_{k1}}{2}}\frac{dl_1\bullet dl_2}{\sqrt{\left[x_3-(x'_3+\Delta x)\right]^2+\Delta_3^2+[z_3+(j-1)(d_U+r)]^2}} \\
\Delta_3 = y_3 - \left[y'_3 + (k-1)(d_R+r)\right]
\end{cases}
\tag{8}
$$

In addition, these mutual inductances are calculated under each sub-coordinate, so in order to utilize the original coordinate, XYZ, to describe the analytical relationship between each mutual inductance and the misaligned position of the receiving coil, the coordinate transformation of each sub-coordinate is necessary.

$$
\begin{bmatrix} x \\ y \\ z \end{bmatrix} =
\begin{bmatrix}
e_x^T e'_x & e_x^T e'_y & e_x^T e'_z \\
e_y^T e'_x & e_y^T e'_y & e_y^T e'_z \\
e_z^T e'_x & e_z^T e'_y & e_z^T e'_z
\end{bmatrix}
\begin{bmatrix} X \\ Y \\ Z \end{bmatrix}
\tag{9}
$$

where $e$ represents the corresponding unit vector.

Thus, $M_{R\text{-}U}$ can be obtained as follow:

$$
\begin{cases}
M_{1(R-U)} = M_{an1-bk1} + M_{an1-bk3} + M_{an2-bk2} + M_{an2-bk4} \\
\qquad + M_{an3-bk1} + M_{an3-bk3} + M_{an4-bk2} + M_{an4-bk4} \\
M_{2(R-U)} = M_{am1-bk1} + M_{am1-bk3} + M_{am3-bk1} + M_{am3-bk3} \\
M_{3(R-U)} = M_{aj1-bk1} + M_{aj1-bk3} + M_{aj2-bk2} + M_{aj2-bk4} \\
\qquad + M_{aj3-bk1} + M_{aj3-bk3} + M_{aj4-bk2} + M_{aj4-bk4} \\
M_{R-U} = M_{1(R-U)} + M_{2(R-U)} + M_{3(R-U)}
\end{cases}
\tag{10}
$$

Furthermore, the corresponding load output voltages when four U-shaped coils work independently can be expressed as

$$
V_{oi} = \frac{\pi^2 M_{R-Ui} U_i}{8 L_i} \quad (i = 1,\ 2,\ 3,\ 4)
\tag{11}
$$

We can indicate that due to the structural characteristics of the four U-shaped coils, the mutual inductances between them and the receiving coil are different when the receiving coil is misaligned. This conclusion also provides the feasibility of the proposed positioning method.

## 4. Positioning Approach

### 4.1. Mutual Inductance Analysis under Different Misalignment

The quadruple-U auxiliary structure is placed directly below the transmitting coil so that once the receiving coil is aligned with the transmitting coil, it is also directly above the center of the auxiliary structure. When the receiving coil is aligned, the variation of four mutual inductances, $M_{R1}$, $M_{R2}$, $M_{R3}$, and $M_{R4}$, with $\Delta X$ and $\Delta Y$, is shown in Figure 9. It can be seen that once the receiving coil is aligned with the quadruple-U auxiliary structure, the coupling degree between the receiving coil and the four U-shaped coils is the same so that the corresponding mutual inductances satisfy the relationship that $MR1 = MR2 = MR3 = MR4$, while if the receiving coil is in a certain misalignment, the numerical value of the corresponding four mutual inductances is different; that is, $MR1 \neq MR2 \neq MR3 \neq MR4$. This is due to the four different coupling degrees caused by the different relative positions between the receiving coil and each U-shaped coil. Meanwhile, take the structure center of each U-shaped coil as the origin, the direction perpendicular to the coil is the X-axis, and the direction horizontal to the coil is the Y-axis, establishing the corresponding four coordinates. We can find that the overall variation of the four mutual inductances is consistent.
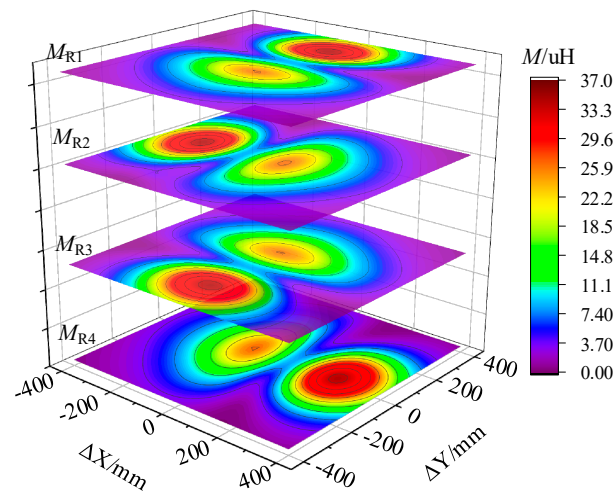


**Figure 9.** $M_{R1}$, $M_{R2}$, $M_{R3}$, and $M_{R4}$ vary with $\Delta X$ and $\Delta Y$.

In addition, the induction range of each U-shaped coil can be obtained by focusing on the variation of each mutual inductance when the receiving coil is nearly aligned, as shown in Table 2.

**Table 2.** Induction range of each U-shaped coil.

| Coil | Induction Range (about the Aligned Position) | Induction Range (Avoid the Aligned Position) |
|---|---|---|
| U1 | −300 mm < $\Delta X$ < 300 mm, −300 mm < $\Delta Y$ < 100 mm | −300 mm < $\Delta X$ < 300 mm, 100 mm < $\Delta Y$ < 500 mm |
| U2 | −100 mm < $\Delta X$ < 300 mm, −300 mm < $\Delta Y$ < 300 mm | −500 mm < $\Delta X$ < −100 mm, −300 mm < $\Delta Y$ < 300 mm |
| U3 | −300 mm < $\Delta X$ < 300 mm, −100 mm < $\Delta Y$ < 300 mm | −300 mm < $\Delta X$ < 300 mm, −500 mm < $\Delta Y$ < −100 mm |
| U4 | −300 mm < $\Delta X$ < 100 mm, −300 mm < $\Delta Y$ < 300 mm | 100 mm < $\Delta X$ < 500 mm, −300 mm < $\Delta Y$ < 300 mm |

Combined with the theoretical analysis and simulation results, we can conclude that when the receiving coil is misaligned, each mutual inductance will change accordingly, which is intuitively manifested as each load voltage changes when the four U-shaped coils work independently.

Taking the U1 coil work independently as an example to illustrate the relationship between the misalignment position of the receiving coil, the mutual inductance $M_{R1}$, and the load voltage $V_{O1}$. When the receiving coil is misaligned, the load voltage can be obtained, and it will correspond to the unique mutual inductance, $M_{R1}$. According to the variation of $M_{R1}$, all of the possible misaligned positions of the receiving coil can be summarized as a specific trajectory in the plane of XOY when the $M_{R1}$ keeps constant, which means that a certain $M_{R1}$ will correspond to countless kinds of receiving coil misalignment cases. Figure 10 is the schematic diagram of the specific trajectory mentioned above.
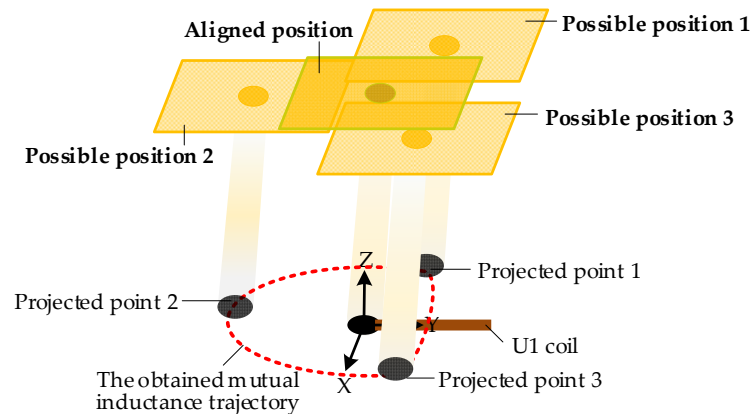


**Figure 10.** Schematic diagram of the specific trajectory.

*4.2. Positioning Approach*

Once the receiving coil is misaligned with the quadruple-U auxiliary structure, the four determined load voltages can be detected; then, the specific mutual inductance trajectories are obtained accordingly. Furthermore, we can deduce the current misalignment position of the receiving coil through the intersection point of the four mutual inductance trajectories. In addition, it is worth noting that the accurate position of the receiving coil can be uniquely determined by the intersection of any three trajectories.

However, due to the misalignment position of the receiving coil being different, there will be two cases of no intersection and one intersection point between the four trajectories. No intersection occurs when the receiving coil is completely outside the identification range of each U-shaped coil or only within one of the coils, which leads to it is impossible to deduce the misalignment position; an intersection occurs when the receiving coil is in the identification range of three or four U-coils, which means that the position of the receiving coil can be accurately obtained. The identifiable range of each coil mentioned is the induction range of them. Thus, in order to deduce the possible positions of the receiving coil, we analyzed the identifiable range of the auxiliary structure in combination with the induction range of each U-shaped coil, as shown in Figure 11.
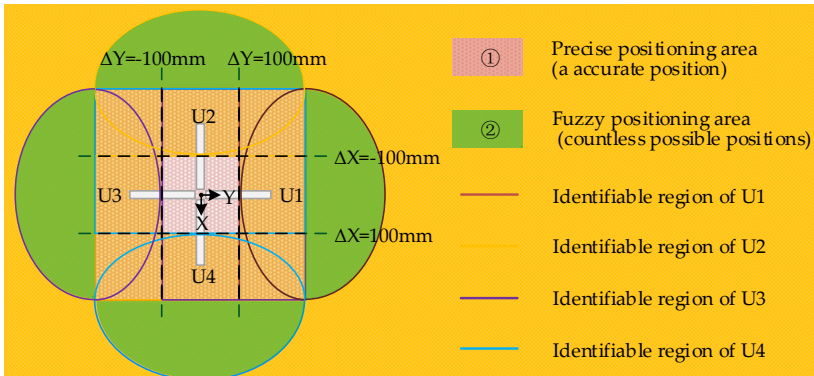


**Figure 11.** Schematic diagram of the identifiable range division.

According to the region division, the positioning function of the receiving coil based on this auxiliary structure can be subdivided into precise positioning and fuzzy positioning.

- Precise Positioning. Through the coupling relationship between the receiving coil and the three or four U-coils, the misalignment position can be determined quickly and accurately. Then the driver decides whether they need to correct the vehicle by using the feedback of the misalignment position.
- Fuzzy Positioning. Through these coupling relationships, only the possible positions in the general area of the receiving coil offset can be predicted. Then, the driver corrects the vehicle into the precise positioning area by using the feedback of the deduced position or area.

Therefore, combined with the specific relationship between the misalignment position, mutual inductances, and load voltages, we proposed a positioning approach by establishing a database in advance and then comparing the measured results and database information to retrieve the misalignment position. Figure 12 is the schematic diagram of the positioning approach of the receiving coil based on the proposed quadruple-U auxiliary structure, and in order to ease the description, we defined the four mutual inductance trajectories obtained through four load voltages as trajectories A, B, C, and D.
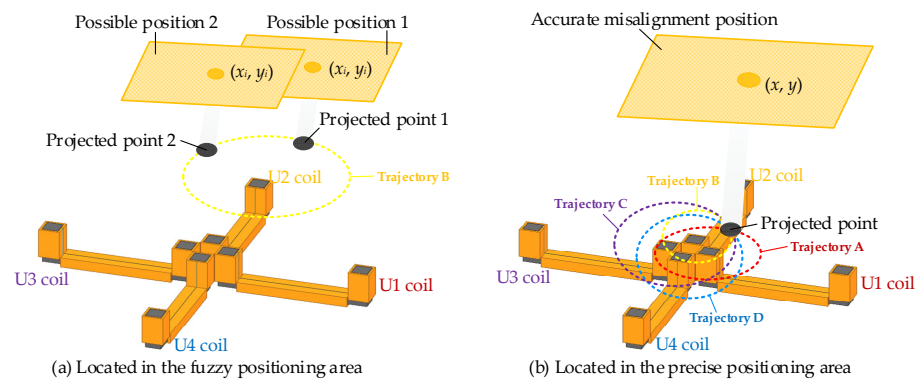


**Figure 12.** Schematic diagram of the positioning approach based on the quadruple-U structure.

Combining the schematic diagram of the positioning process mentioned above and the flowchart shown in Figure 13, the entire process of the receiving coil positioning can be described in four steps.
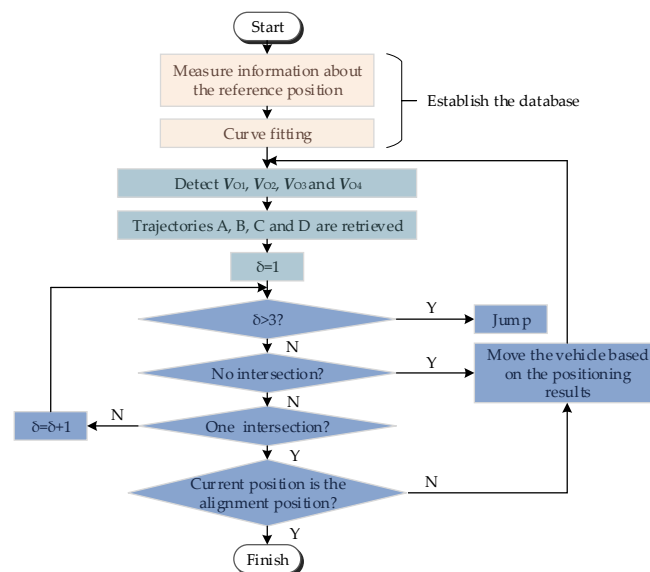


**Figure 13.** Flowchart of the proposed method.

Step I: The load voltages and mutual inductances are measured at the reference positions, and a database is formed by fitting these data. In addition, the move step of the reference position is 20 mm.

Step II: When the receiving coil enters the identifiable area of any U-shaped coil, the load voltages of the four U-coils working independently are measured. By comparing the measured information with the database information, the best matching four mutual inductance trajectories, A, B, C, and D, are retrieved.

Step III: If there is no intersection between A, B, C, and D, it means that only one U-shaped coil can identify the receiving coil, and then feedback the results to the driver. Moreover, if there is only one intersection point $(x, y)$ between them, which can be regarded as the accurate position of the receiving coil. At this time, we need to judge whether the position is the alignment position $(0, 0)$. If so, the positioning state will be terminated; if not, the driver removes the vehicle according to the feedback of the positioning results.

Step IV: Move the vehicle according to the feedback of the positioning results, and repeat step II and step III until the receiving coil is aligned with the auxiliary structure.

Furthermore, in order to avoid the comparison program from entering a dead loop and being unable to achieve real-time positioning and guidance, a jump program is introduced. Once the repeated judgment times, δ, of the same position exceed three, the program jumps out of the loop and detects the load voltage again by the MCU to realize the receiving coil positioning.

## 5. Experimental Validation

A wireless charging system prototype with the proposed quadruple-U auxiliary structure LCC-S compensation circuit was built and tested to illustrate the positioning feasibility of the proposed novel structure. The quadruple-U auxiliary structure and the experimental prototype are shown in Figure 14a,b, respectively. The former consists of four U-shaped coils arranged symmetrically in cruciform, and the parameters of each component involved in the latter are listed in Table 3.



(a) Quadruple-U auxiliary structure  (b) Experimental prototype
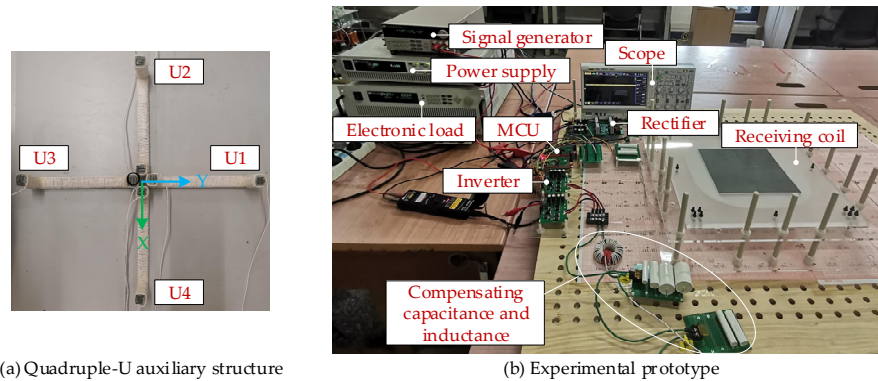
**Figure 14.** Experimental prototype.

**Table 3.** Parameters of WPT positioning system.

| Parameter | Value | Parameter | Value | Parameter | Value |
|---|---|---|---|---|---|
| MCU | TMS320F28335 | $C_1$ | 126.5/nF | $C_3$ | 126.5/nF |
| $S_1$–$S_4$ | SiHB33N60EF | $L_{U2}$ | 722.8/μH | $L_{U4}$ | 717.6/μH |
| $D_1$–$D_4$ | IDW20G65C5 | $L_2$ | 20.4/μH | $L_4$ | 20.4/μH |
| $L_R$ | 409.5/μH | $C_{U2}$ | 2.87/nF | $C_{U4}$ | 4.4/nF |
| $C_R$ | 7.7/nF | $C_2$ | 126.5/nF | $C_4$ | 126.5/nF |
| $L_{U1}$ | 720.1/μH | $L_{U3}$ | 718.7/μH | $C_O$ | 220/μF |
| $L_1$ | 20.4/μH | $L_3$ | 20.4/μH | $R$ | 5000/Ω |
| $C_{U1}$ | 4.2/nF | $C_{U3}$ | 4.3/nF | $f_O$ | 95/kHz |

### 5.1. Verification of Mutual Inductance

Combined with the symmetry of the quadruple-U structure, we verified the relationship that $M_{R1}$, $M_{R2}$, $M_{R3}$, and $M_{R4}$ vary with the misalignment of the receiving coil just by measuring each mutual inductance in a certain quadrant of the XOY plane when the receiving coil is misaligned. Hence, an array of $7 \times 9$ typical positions within the identifiable range that abut the aligned position of each U-shaped coil was measured. The experimental results of the four mutual inductances in the misalignment cases are shown in Figure 15a–d.
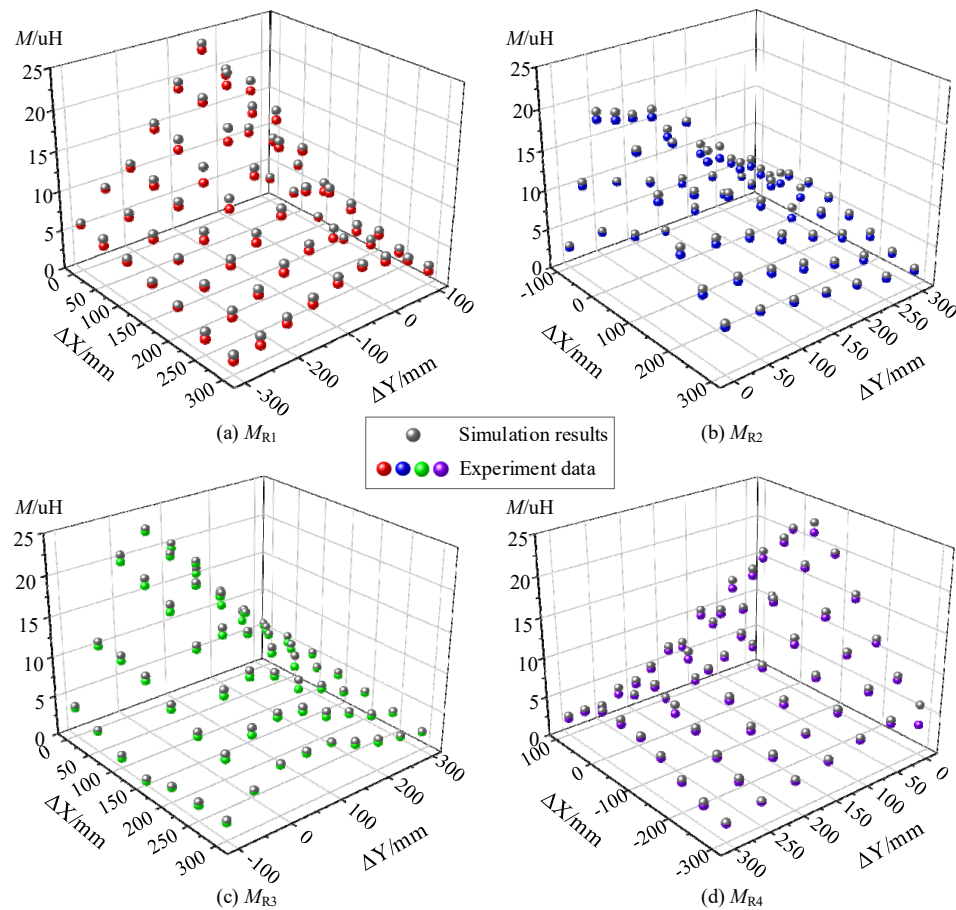


**Figure 15.** Simulation results and experimental data of $M_{R1}$, $M_{R2}$, $M_{R3}$, and $M_{R4}$.

As shown in Figure 15a, it can be seen that within the test range of the U1 coil, the numerical value of the mutual inductance, $M_{R1}$, presents a variation of gradually increasing to the maximum and then decreasing with $\Delta Y$, and there is an inverse relationship between $M_{R1}$ and $\Delta X$, which are consistent with the variation obtained by the simulation. In addition, according to the symmetry of the magnetic field of the U1 coil shown in Figure 9, we can deduce that when $\Delta X \in [-300 \text{ mm}, 0 \text{ mm}]$ and $\Delta Y \in [-300 \text{ mm}, 100 \text{ mm}]$, the variation of $M_{R1}$ with $\Delta Y$ is consistent with that in Figure 15a, while the variation of $M_{R1}$ with $\Delta X$ is opposite of that in Figure 15a. Therefore, combining the symmetry of the structure and the test results, we can indicate that there exists a symmetry among the four mutual inductions, $M_{R1}$, $M_{R2}$, $M_{R3}$, and $M_{R4}$. Moreover, the numerical value of the measured mutual inductances is slightly smaller than those in the simulations, and the deviations are less than 10%. The tiny differences are caused by the ferrite of the U-shaped coil being composed of a few ferrites with different sizes overlapping and splicing together.

## 5.2. Verification of Load Voltage

In the actual parking process, the parking direction points to the *X*-axis, generally after installing the quadruple-U auxiliary structure. Hence, it is necessary to position the receiving coil and feedback the result to the driver for assistance in the parking process when the misalignment position of the receiving coil is in the second or third quadrants of the XYZ coordinate. Considering the identifiable range of each U-shaped coil within the range of $\Delta X \in [-300 \text{ mm}, 0 \text{ mm}]$ and $\Delta Y \in [-300 \text{ mm}, 300 \text{ mm}]$, we measured the load voltages of several typical positions when the misalignment step of the receiving coil was 50 mm. These voltages were detected when each U-shaped coil worked independently under the condition that the transmission distance was fixed at 160 mm. The measurement results of each load voltage are shown in Figure 16.
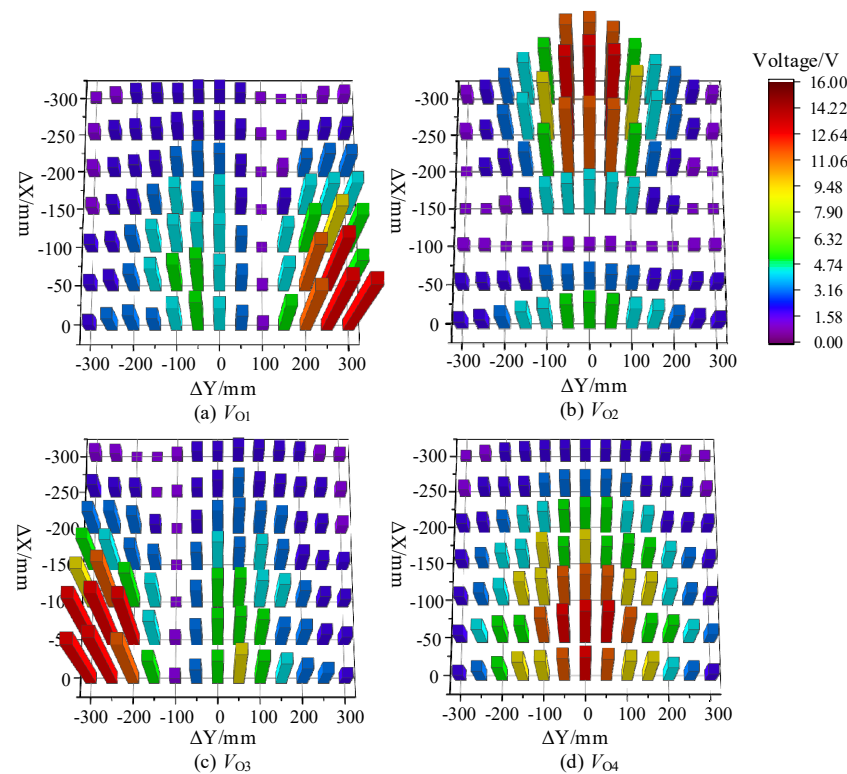


**Figure 16.** Measurement results of $V_{O1}$, $V_{O2}$, $V_{O3}$, and $V_{O4}$.

On the one hand, it can be seen from the load voltage measurement results that once the receiving coil is offset, the load voltages obtained under the condition that the four U-shaped coils work independently are different, which verifies the feasibility of the proposed approach of positioning the receiving coil by three or four load voltages. On the other hand, within the test range, the identifiable ranges of the U1 coil, U2 coil, U3 coil, and U4 coil are $\Delta X \in [-300 \text{ mm}, 0 \text{ mm}] \cap \Delta Y \in [-300 \text{ mm}, 300 \text{ mm}]$ (except for $\Delta Y = 100 \text{ mm}$), $\Delta X \in [-300 \text{ mm}, 0 \text{ mm}] \cap \Delta Y \in [-300 \text{ mm}, 300 \text{ mm}]$ (except for $\Delta X = -100 \text{ mm}$), $\Delta X \in [-300 \text{ mm}, 0 \text{ mm}] \cap \Delta Y \in [-300 \text{ mm}, 300 \text{ mm}]$ (except for $\Delta Y = -100 \text{ mm}$), and $\Delta X \in [-300 \text{ mm}, 0 \text{ mm}] \cap \Delta Y \in [-300 \text{ mm}, 300 \text{ mm}]$. Meanwhile, the U-shaped coil can be considered a bipolar coil, for it is inspired by the solenoid coil, while the rectangular receiving coil is a unipolar coil, resulting in decoupling between them. Hence, these special cases are due to the fact that the receiving coil is misaligned above the structural center of a certain U-shaped coil; that is, the magnetic field between them is decoupled. Furthermore, according to the symmetry of the quadruple-U auxiliary structure and these measurements, the identifiable range of each U-shaped coil in the first and fourth quadrants of the XYZ coordinate can be deduced. Eventually, combined with the symmetry of the structure and test results, we can conclude that the identifiable range of the designed

quadruple-U auxiliary structure can reach $\Delta X \in [-300$ mm, 300 mm$] \cap \Delta Y \in [-300$ mm, 300 mm], which also verifies the accuracy of the identifiable range division mentioned in the theoretical analysis.

*5.3. Positioning Results*

The various positions of the receiving coil distributed throughout the $\Delta X \in [-100$ mm, 100 mm$] \cap \Delta Y \in [-100$ mm, 100 mm] range with a fixed 160 mm transmission distance were tested to verify the proposed positioning approach. Figure 17 illustrates the positioning results in typical positions; the square points marked in blue and the triangular points marked in red represent the calibration values and measured results, respectively. The receiving coil was placed at each typical position, and the proposed positioning process was carried out. At each of the test points, the load voltages $V_{O1}$, $V_{O2}$, $V_{O3}$, and $V_{O4}$ were measured when the four U-shaped coils worked independently, and the intersection point coordinates were deduced after obtaining the most matched information by retrieving these load voltages from the database. As shown in Figure 14, the proposed positioning method based on the special quadruple-U auxiliary structure exhibits a wide positioning range and high positioning accuracy. On the one hand, among the $6 \times 6$ and $4 \times 7$ tested positions, all of them were accurate to within 10 mm. On the other hand, combined with the symmetry of the auxiliary structure and the obtained identifiable range within $\Delta X \in [-300$ mm, 0 mm$] \cap \Delta Y \in [-300$ mm, 300 mm], we can conclude that the overall identifiable range of the designed auxiliary structure is $\Delta X \in [-300$ mm, 300 mm$] \cap \Delta Y \in [-300$ mm, 300 mm].
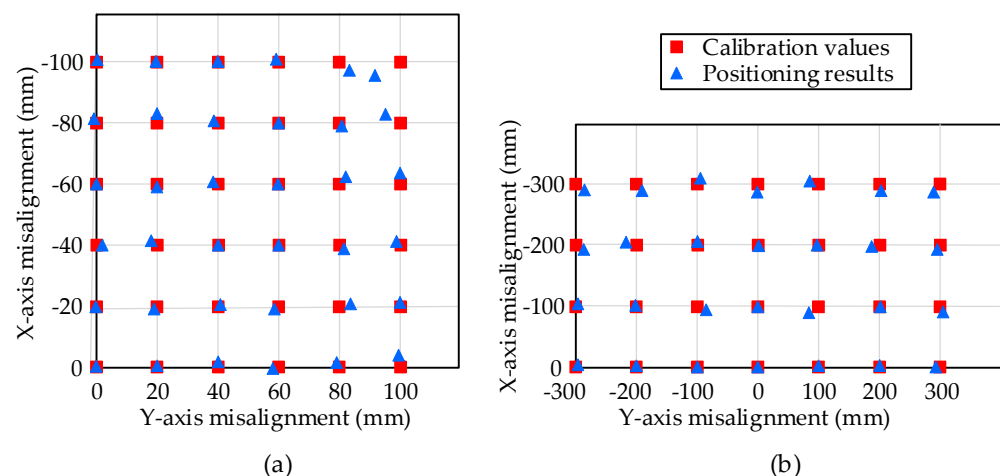


**Figure 17.** Positioning results in typical positions. (**a**) The moving step of the receiving coil is 20 mm. (**b**) The moving step of the receiving coil is 100 mm.

## 6. Conclusions

In this paper, a receiving coil positioning method integrated with a novel quadruple-U auxiliary structure is proposed. By using the inverter configured in the wireless charging system and the receiving coil installed in the vehicle, the receiving coil is positioned before the wireless power transmission process to ensure that the receiving coil is located in the effective charging area. Compared to the prior positioning methods based on the auxiliary structure, the designed quadruple-U auxiliary structure and the proposed positioning approach have the advantages of wider positioning ranges, higher positioning accuracy, and not changing the structure of the receiving coil. An experimental prototype was realized, and the feasibility of the proposed positioning approach was demonstrated. The experimental results indicate that all of the tested positions are accurate to within 10 mm, with a 160 mm transfer distance. Meanwhile, combined with the symmetry of the auxiliary structure and the test results, it can be indicated that the positioning range can reach $\Delta X \in [-300$ mm, 300 mm$] \cap \Delta Y \in [-300$ mm, 300 mm].

## References

1. Limb, B.J.; Asher, Z.D.; Bradley, T.H.; Sproul, E.; Trinko, D.A.; Crabb, B.; Zane, R.; Quinn, J.C. Economic viability and environmental impact of in-motion wireless power transfer. *IEEE Trans. Transp. Electrif.* **2019**, *5*, 135–146. [CrossRef]
2. Zhang, Z.; Pang, H.; Georgiadis, A.; Cecati, C. Wireless Power Transfer—An Overview. *IEEE Trans. Ind. Electron.* **2019**, *66*, 1044–1058. [CrossRef]
3. Yang, Y.; Zhang, X.; Luo, L.; Xie, S.; Zhou, Q. Research on high power factor single tube variable structure wireless power transmission. *World Electr. Veh. J.* **2021**, *12*, 214. [CrossRef]
4. Javan-Khoshkholgh, A.; Farajidavar, A. Simultaneous Wireless Power and Data Transfer: Methods to Design Robust Medical Implants for Gastrointestinal Tract. *IEEE J. Electromagn. RF Microw. Med. Biol.* **2022**, *6*, 3–15. [CrossRef]
5. Roy, S.; Azad, A.W.; Baidya, S.; Alam, M.K.; Khan, F. Powering Solutions for Biomedical Sensors and Implants Inside the Human Body: A Comprehensive Review on Energy Harvesting Units, Energy Storage, and Wireless Power Transfer Techniques. *IEEE Trans. Power Electron.* **2022**, *37*, 12237–12263. [CrossRef]
6. Loewel, T.; Lange, C.; Noack, F. Identification and Positioning System for Inductive Charging Systems. In Proceedings of the 2013 3rd International Electric Drives Production Conference (EDPC), Nuremberg, Germany, 29–30 October 2013; pp. 1–5.
7. Zucca, M.; Squillari, P.; Pogliano, U. A Measurement System for the Characterization of Wireless Charging Stations for Electric Vehicles. *IEEE Trans. Instrum. Meas.* **2021**, *70*, 9001710. [CrossRef]
8. Zhou, Y.; Law, C.L.; Guan, Y.L.; Chin, F. Indoor Elliptical Localization Based on Asynchronous UWB Range Measurement. *IEEE Trans. Instrum. Meas.* **2011**, *60*, 248–257. [CrossRef]
9. Pan, Z.; Yang, X.; Wang, C.; Fei, Y.; Xu, Q.; Li, C. Research on coil positioning technology based on BP neural network. *Electr. Meas. Instrum.* **2021**, *12*, 1–8. Available online: http://kns.cnki.net/kcms/detail/23.1202.TH.20211201.2306.002.html (accessed on 7 March 2023). (In Chinese).
10. Li, Y.; Jiang, X.; Ying, Y.; Xie, K. Research on Coil Self-Positioning Method for Inductive Wireless Power Supply System. pp. 1–11. Available online: http://kns.cnki.net/kcms/detail/11.2107.TM.20220324.1656.015.html (accessed on 7 March 2023). (In Chinese).
11. Feng, H.; Tavakoli, R.; Onar, O.C.; Pantic, Z. Pantic, Advances in High-Power Wireless Charging Systems: Overview and Design Considerations. *IEEE Trans. Transp. Electrif.* **2020**, *6*, 886–919. [CrossRef]
12. Khan, N.; Matsumoto, H.; Trescases, O. Wireless Electric Vehicle Charger with Electromagnetic Coil-Based Position Correction Using Impedance and Resonant Frequency Detection. *IEEE Trans. Power Electron.* **2020**, *35*, 7873–7883. [CrossRef]
13. Zhang, Z.; Zheng, S.; Yao, Z.; Xu, D.; Krein, P.T.; Ma, H. A Coil Positioning Method Integrated with an Orthogonal Decoupled Transformer for Inductive Power Transfer Systems. *IEEE Trans. Power Electron.* **2022**, *37*, 9983–9998. [CrossRef]
14. Senju, R.; Omori, H.; Uchimoto, D.; Morizane, T.; Kimura, N. A New Position Detecting Method for Wireless EV Chargers. In Proceedings of the 2019 8th International Conference on Renewable Energy Research and Applications (ICRERA), Brasov, Romania, 3–6 November 2019; pp. 810–814.
15. Feng, T.; Zuo, Z.; Sun, Y.; Dai, X.; Wu, X.; Zhu, L. A Reticulated Planar Transmitter Using a Three-Dimensional Rotating Magnetic Field for Free-Positioning Omnidirectional Wireless Power Transfer. *IEEE Trans. Power Electron.* **2022**, *37*, 9999–10015. [CrossRef]
16. Jeong, S.Y.; Kwak, H.G.; Jang, G.C.; Choi, S.Y.; Rim, C.T. Dual-Purpose Nonoverlapping Coil Sets as Metal Object and Vehicle Position Detections for Wireless Stationary EV Chargers. *IEEE Trans. Power Electron.* **2018**, *33*, 7387–7397. [CrossRef]
17. Gao, Y.; Duan, C.; Oliveira, A.A.; Ginart, A.; Farley, K.B.; Tse, Z.T.H. 3-D Coil Positioning Based on Magnetic Sensing for Wireless EV Charging. *IEEE Trans. Transp. Electrif.* **2017**, *3*, 578–588. [CrossRef]
18. Wang, W.; Zhang, C.; Wang, J.; Tang, X. Multipurpose Flexible Positioning Device Based on Electromagnetic Balance for EVs Wireless Charging. *IEEE Trans. Ind. Electron.* **2021**, *68*, 10229–10239. [CrossRef]
19. Tan, L.; Li, C.; Li, J.; Wang, R.; Huang, T.; Li, H.; Huang, X. Mesh-Based Accurate Positioning Strategy of EV Wireless Charging Coil with Detection Coils. *IEEE Trans. Ind. Inform.* **2021**, *17*, 3176–3185. [CrossRef]
20. Yang, Y.; Cao, G.; Zhang, G.; Xie, S. Wireless Power Transfer Positioning System with Wide Range Direction-Guided Based on Symmetrical Triple-U Auxiliary Pad. *World Electr. Veh. J.* **2022**, *13*, 140. [CrossRef]

21.    Liu, S.; Su, J.; Lai, J.; Zhang, J.; Xu, H. Precise Modeling of Mutual Inductance for Planar Spiral Coils in Wireless Power Transfer and Its Application. *IEEE Trans. Power Electron.* **2021**, *36*, 9876–9885. [CrossRef]
22.    Pirinççi, N.; Altun, H. A New Analytical Study on Mutual Inductance Calculations for Wireless Power Transfer Using Magnetic Vector Potential. *IEEE Trans. Magn.* **2022**, *58*, 1–14. [CrossRef]
23.    Chen, X.; Wu, L.; Zhang, J. Theoretical analysis and discussion of magnetic field of current carrying coil and finite length straight solenoid. *Coll. Phys.* **2019**, *38*, 23–27. (In Chinese)
24.    Zhou, X.; Liu, S.; Zhang, S.; Sun, M.; Lu, J.; Huang, D. Theoretical analysis and visual study of magnetic field uniformity distribution of finite length solenoid. *Coll. Phys.* **2021**, *40*, 76–81. (In Chinese)
25.    Zhang, X.; Quan, C.; Li, Z. Mutual Inductance Calculation of Circular Coils for an Arbitrary Position with Electromagnetic Shielding in Wireless Power Transfer Systems. *IEEE Trans. Transp. Electrif.* **2021**, *7*, 1196–1204. [CrossRef]
26.    Xu, S.; Zhang, H.; Yao, C.; Tang, H.; Ma, D. Fine Positioning Method for Wireless Charging System of Electric Vehicles. *Instrum. Tech. Sens.* **2020**, *2020*, 59–63. (In Chinese)
27.    Hao, S.; Li, B. Calculation Inductance of Toroidal Inductor Wound by Rectangular Cross-Sectional Wire. *IEEE Trans. Plasma Sci.* **2021**, *49*, 2910–2915. [CrossRef]